the microreactor, and subsequently in 5×10^{-4} torr of flowing H_2 for another 5 min to remove all surface oxygen. Thermal desorption spectra of CO from the surface, which were in complete agreement with previously published ones from the clean Pt(110)-(1 × 2) surface [C. M. Comrie and R. M. Lambert, *J. Chem. Soc. Faraday Trans.* **72**, 325 (1975)], were measured frequently in order to verify the cleanliness of the surface. Furthermore, all of the data concerning propane activation presented here were reproducible, indicating the absence of surface contamination. The C_3H_8 (99.5%) was obtained from Matheson, and both the $CH_3CD_2CH_3$ (98% by atom D) and the C_3D_8 (99.5% by atom D) were obtained from MSD Isotopes. All gases were stored and manipulated in a manifold that was pumped by a diffusion pump and which had a base pressure below 10^{-7} torr.

21. Under these experimental conditions the dissociative chemisorption of propane is irreversible, and no gas-phase carbon-containing products of a surface self-hydrogenolysis reaction are produced.
22. Note also that the observed kinetic isotope effect implies that C–H rather than C–C bond cleavage is occurring in the initial dissociative chemisorption, as would be expected. Furthermore, we have shown previously that the initial C–H bond-cleavage reaction is rate limiting in alkane activation (*9, 10, 17*).
23. If curved Arrhenius constructions are observed, then the raw data may be used directly to extract E_{r1} and E_{r2} via Eq. 4.
24. The support of this work by the Department of Energy (grant DE-FG03-89ER14048) and the Donors of The Petroleum Research Fund administered by the American Chemical Society (grant ACS-PRF-23801-AC5-C) is gratefully acknowledged.

15 April 1991; accepted 17 June 1991

Dimerization of Human Growth Hormone by Zinc

BRIAN C. CUNNINGHAM, MICHAEL G. MULKERRIN, JAMES A. WELLS*

Size-exclusion chromatography and sedimentation equilibrium studies demonstrated that zinc ion (Zn^{2+}) induced the dimerization of human growth hormone (hGH). Scatchard analysis of $^{65}Zn^{2+}$ binding to hGH showed that two Zn^{2+} ions associate per dimer of hGH in a cooperative fashion. Cobalt (II) can substitute for Zn^{2+} in the hormone dimer and gives a visible spectrum characteristic of cobalt coordinated in a tetrahedral fashion by oxygen- and nitrogen-containing ligands. Replacement of potential Zn^{2+} ligands (His^{18}, His^{21}, and Glu^{174}) in hGH with alanine weakened both Zn^{2+} binding and hGH dimer formation. The Zn^{2+}-hGH dimer was more stable than monomeric hGH to denaturation in guanidine-HCl. Formation of a Zn^{2+}-hGH dimeric complex may be important for storage of hGH in secretory granules.

HUMAN GROWTH HORMONE (hGH) is synthesized and secreted into storage granules before its release from the anterior pituitary (*1, 2*). Histochemical analysis of the anterior pituitary indicates that Zn^{2+} is present in high concentrations in growth hormone secretory granules (*3*). It has been suggested that Zn^{2+} may modulate release of growth hormone because high concentrations of Zn^{2+} inhibit growth hormone release (*4–6*). However, the biochemical and structural basis whereby Zn^{2+} functions in storage or release of hGH has not been elucidated.

After analyzing the binding of Zn^{2+} in the complex between hGH and the extracellular domain of the human prolactin receptor (hPRLbp) [K_d (dissociation constant) = 0.03 nM] (*7*), we measured the binding affinity of Zn^{2+} to each protein separately. Equilibrium dialysis showed no specific binding of $^{65}Zn^{2+}$ to the hPRLbp, whereas Scatchard analyses of binding studies performed at two different concentrations of hGH (3.3 μM and 4.8 μM) showed that Zn^{2+} forms a 1:1 complex with hGH (Fig. 1). The Scatchard plots curved upward, indicating that binding of one Zn^{2+} ion promotes the binding of another Zn^{2+} ion (positive cooperativity). From the linear portions of these plots, we estimate an apparent K_d for the higher affinity Zn^{2+} site of about 1 μM. Cooperative binding with a stoichiometry of 1:1 could be explained if Zn^{2+} induced hGH to oligomerize.

We used size exclusion chromatography to determine if Zn^{2+} did indeed induce oligomerization of hGH. Gel filtration of hGH (15 μM) in EDTA (Fig. 2) showed that hGH elutes as a symmetrical peak at a position corresponding to a molecular size of ~20 kD, approximately the size of monomeric hGH (22 kD). However, in the presence of $ZnCl_2$ (50 μM) the hormone chromatographed with an apparent molecular size that is 50% larger than in EDTA. The asymmetry of this peak is characteristic of a species that is dissociating on the column (*8*). At higher concentrations of hGH and $ZnCl_2$ (~150 μM), the hGH chromatographed as a more symmetrical peak with an apparent molecular size that is 1.85 times the monomeric hGH peak (*9*). Thus, at higher concentrations the dimerization is essentially complete. At lower concentrations (0.15 μM), hGH runs only as a monomer (*9*). These data indicate that at concentrations of hGH greater than micromolar, Zn^{2+} is able to promote the formation of an hGH dimer.

Sedimentation equilibrium studies (Fig. 3) confirm that hGH forms a dimeric complex (~44 kD) in the presence of, but not in the absence of, $ZnCl_2$. Moreover, the concentration dependence for dimer formation allowed us to calculate an apparent dimerization equilibrium constant for hGH (± SD) of 2.6 ± 0.1 μM in 20 μM $ZnCl_2$ (Table 1).

To probe the structural environment of the Zn^{2+} sites in the hGH dimer, we substituted Co^{2+}, a spectroscopically active metal (*10, 11*), for Zn^{2+}. Gel filtration experiments showed that Co^{2+} also induces dimerization of hGH (*9*). Moreover, both Zn^{2+} and Co^{2+} produce similar ultraviolet difference spectra on dimerization of the hormone (*9*), suggesting that the Zn^{2+} and Co^{2+} hGH complexes are structurally similar, if not identical.

Titration of hGH with Co^{2+} produces a visible absorption spectrum with a maxi-

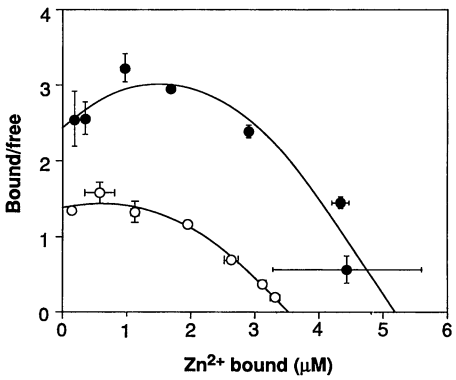

Fig. 1. Equilibrium dialysis and Scatchard analysis for binding of $^{65}Zn^{2+}$ to hGH (○, 3.3 μM; ●, 4.8 μM). We took precautions to minimize Zn^{2+} contamination in the buffers and dialysis cells as described (*7*). The hGH was mixed with dialysis buffer that contained tris, pH 7.5 (20 mM); NaCl (140 mM); and $MgCl_2$ (10 mM). We added the $MgCl_2$ to reduce nonspecific binding of Zn^{2+} to the dialysis cell membrane and hGH. The $MgCl_2$ neither promoted nor inhibited dimerization of hGH (*9*). Aliquots (100 μl) of the solution that contained hGH (3.3 or 4.8 μM) were added to one side of the dialysis cell. Serial dilutions (in triplicate) of unlabeled $ZnCl_2$ that contained 0.3 μM $^{65}ZnCl_2$ (eight dilution steps ranging from 0 to a final $ZnCl_2$ concentration of 40 μM) were added to the other side of the dialysis cell. Cells were rotated slowly for 16 to 20 hours at 25°C. Control experiments indicated this was sufficient time to reach equilibrium. Aliquots (50 μl) from each side of the dialysis cell were diluted into scintillation cocktail and analyzed for $^{65}Zn^{2+}$ content. From these values the concentrations of bound and free Zn^{2+} were calculated. Error bars indicate SD from triplicate determinations.

Department of Protein Engineering, Genentech, South San Francisco, CA 94080.

*To whom correspondence should be addressed.

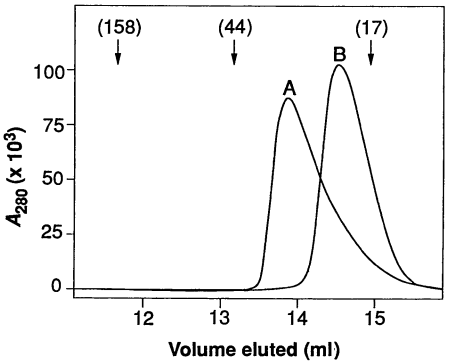

Fig. 2. Gel filtration chromatography of hGH in the presence (curve A) or absence (curve B) of $ZnCl_2$. One hundred microliters of a solution that contained hGH (50 μM); tris, pH 7.5 (20 mM); NaCl (100 mM); and either $ZnCl_2$ (50 μM) or EDTA (1 mM) was applied to a prepacked Superose 12 column (HR 10/30; Pharmacia) equilibrated in each buffer and eluted at 0.35 ml/min with the same buffer without hGH. Peak locations (in kilodaltons) are indicated by arrows at the top of the chromatogram; we determined these locations from size standards (bovine γ-globulin, ovalbumin, and myoglobin, respectively) run separately to calibrate the column. A_{280}, absorbance at 280 nm.

mum at 525 nm and a molar absorptivity of 260 cm^{-1} M^{-1} (Fig. 4), characteristic of Co^{2+} that is in a tetrahedral environment and coordinated by a mixture of nitrogen- and oxygen-containing ligands (*10, 11*). However, the visible circular dichroic spectrum of the Co^{2+}-hGH dimeric complex is virtually flat (*9*), indicating that the bound Co^{2+} is in a symmetrical environment (*11*). This could arise if each Co^{2+} site in the dimer is highly symmetrical or, more likely, if the two Co^{2+} sites are asymmetric; asymmetric sites that are pseudomirror images of each other have dichroic effects equal in magnitude but of opposite sign and thus cancel each other.

We used mutational analysis to further localize the sites of Zn^{2+} coordination in the $(Zn^{2+}\text{-hGH})_2$ complex. Similar studies indicated that His^{18}, His^{21}, and Glu^{174} participate in Zn^{2+}-mediated binding of hGH to the hPRLbp (*7*). Gel filtration studies revealed that mutation of each of these residues to alanine caused reductions in the formation of dimeric hGH (*9*). From the elution of the mutant proteins in the presence of $ZnCl_2$ or EDTA, we determined that the E174A variant gave no indication of dimer formation and that the H21A and H18A mutants exhibited substantially reduced dimer formation.

Sedimentation equilibrium studies allowed us to quantify the effect of mutations that encompass the putative Zn^{2+} site on the dimerization constant of hGH in $ZnCl_2$ (Table 1). The dimerization affinity is about 150-fold greater in the presence of $ZnCl_2$, as compared to EDTA. Mutation of His^{21} or Glu^{174} to alanine reduced the dimer affinities to 1/58 and 1/11 of the wild-type value, respectively. There was no effect from mutation of Asp^{171}, which is near the Zn^{2+} site.

Equilibrium dialysis studies showed that the reduction in dimer formation correlated with a loss in capacity to bind $^{65}Zn^{2+}$ (Table 2). At low concentrations of Zn^{2+}, the ratio of bound to free Zn^{2+} decreases in the following order: hGH ~ D171A >> H21A ~ H18A > E174A. Thus, gel filtration, sedimentation equilibrium, and equilibrium dialysis experiments indicate that His^{18}, His^{21}, and Glu^{174} participate in coordinating Zn^{2+} and promoting formation of the hormone dimer. These residues are positioned in the tertiary structure of hGH (Fig. 5) such that Zn^{2+} may bridge two α-helical segments, as was designed into a four-helix bundle protein (*12*).

Zn^{2+} typically coordinates four ligands in proteins (*13*). Sedimentation equilibrium and Zn^{2+} binding studies indicate that Asp^{171} is not the fourth Zn^{2+} ligand, even

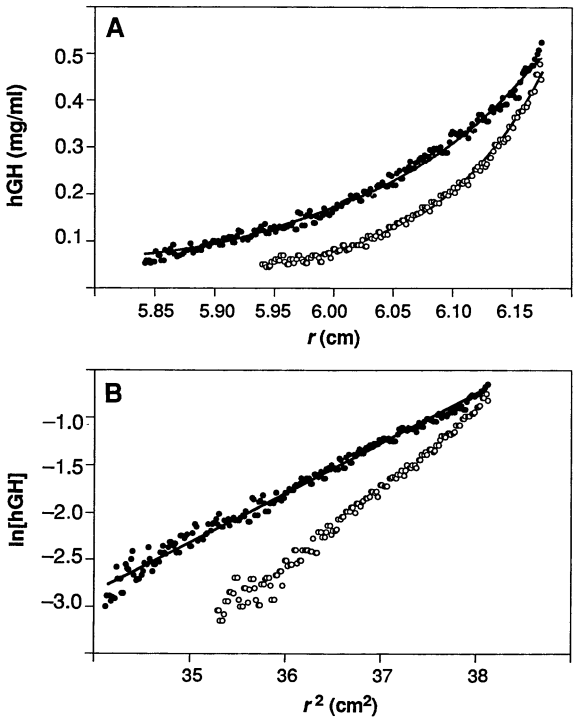

Fig. 3. Sedimentation equilibrium analysis of hGH in the absence (●) or presence (○) of $ZnCl_2$ (20 μM). Samples of hGH (0.2 mg/ml, 0.15 mg/ml, or 0.1 mg/ml) in tris, pH 8.0 (10 mM); and NaCl (0.1 M) with or without $ZnCl_2$ (20 μM) were loaded into a six-channel Yphantis cell (*21*) and centrifuged in a Beckman Model E centrifuge at 20,000 rpm for 48 hours at 20°C. (**A**) The concentration of hGH (initially 0.2 mg/ml) versus radial distance (r) (in centimeters). We fit the combined data for all three hormone concentrations with a computer program (*22*) to a monomer-dimer equilibrium to determine the dimerization constant (K_d = 2.6 μM). (**B**) The graph of the natural log of the hGH concentration versus r^2 is a linear plot in the absence of $ZnCl_2$ (○), in agreement with a plot for a monomeric species.

Table 1. The dimerization constants of hGH and hGH mutants analyzed by analytical sedimentation equilibrium. The analysis of each of these hormones was carried out as described in Fig. 3 in the presence of 20 μM $ZnCl_2$. The SD in the K_d value from two separate determinations for wild-type hGH was ±0.1 μM. Mutants are indicated by the single letter amino acid for the wild-type residue, followed by its position in mature hGH and then the mutant residue. For example, H18A designates a mutant where His^{18} is changed to Ala. Mutants of hGH were expressed in *Escherichia coli* and purified as described (*7, 16, 17*). Abbreviations for the amino acid residues are as follows: A, Ala; C, Cys; D, Asp; E, Glu; F, Phe; G, Gly; H, His; I, Ile; K, Lys; L, Leu; M, Met; N, Asn; P, Pro; Q, Gln; R, Arg; S, Ser; T, Thr; V, Val; W, Trp; and Y, Tyr.

Hormone	K_d (μM)
hGH	2.6
hGH (+ EDTA)	380
H21A	150
E174A	28
D171A	3.9

Table 2. Comparative binding of low concentrations of $ZnCl_2$ (0.6 μM final) to hGH and hGH mutants. Equilibrium dialysis for binding of $^{65}Zn^{2+}$ to hGH and variants of hGH was carried out (n = 2) as described in Fig. 1, except we increased the hormone concentration to 45 μM to enhance the signal and more accurately measure weak binding of Zn^{2+}. The H18A, H21A, D171A, and E174A mutants were prepared and purified as described (*7, 16, 17*).

Hormone	Average (±SD) Zn^{2+} bound/free
Wild type	18.3 ± 4.3
H18A	5.1 ± 0.2
H21A	8.7 ± 1.2
D171A	27.4 ± 0.2
E174A	1.8 ± 0.1

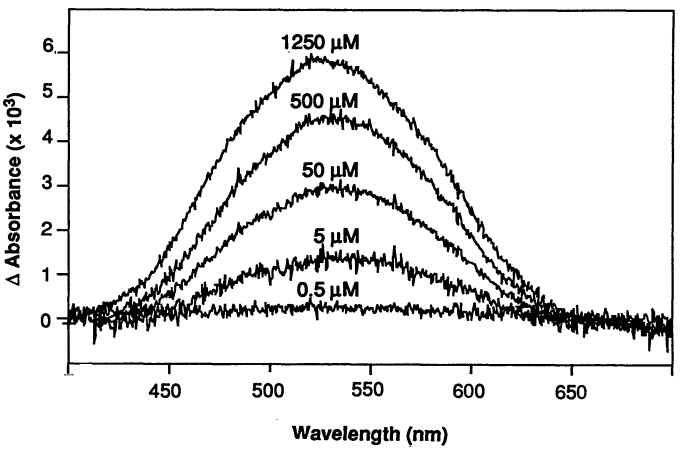

Fig. 4. Visible difference spectra for the binding of increasing concentrations of Co^{2+} to hGH. The hGH concentration was 23 μM and the Co^{2+} concentration ranged from 5 to 1250 μM, as indicated. The molar absorptivity (260 cm^{-1} M^{-1}) was calculated from the maximal change in absorbance at 525 nm ($6 \times 10^{-3} cm^{-1}$), divided by the concentration of hGH in the cuvette (23 μM).

though it is proximal in the folded model of hGH (Fig. 5). Although there are no other nearby side chains that can coordinate Zn^{2+}, it is possible that the fourth Zn^{2+} ligand is a water molecule. Alternatively, His^{18}, His^{21}, or Glu^{174} may bridge two Zn^{2+} ions in the dimer. In this model, the Zn^{2+} ions are sandwiched at the interface and are related by a pseudomirror plane of symmetry. This would explain the absence of a strong Co^{2+} circular dichroic effect in the dimer. Furthermore, the highly cooperative nature of Zn^{2+} binding suggests that the two sites are interdependent.

We propose that the Zn^{2+}-hGH dimer produced here in vitro may be the major storage form of hGH. Most of the Zn^{2+} in the pituitary is located in somatotrophic granules (*3*) along with hGH (*1*) in roughly equimolar amounts (*14*). In addition, the concentration of hGH and Zn^{2+} in the vesicles is probably greater than 1 mM (*14*). This concentration is at least 400-fold greater than the dissociation constant for the Zn^{2+}-hGH dimer (2.6 μM). Virtually all of the hGH could exist as a $(Zn^{2+}\text{-hGH})_2$ complex.

We suggest the $(Zn^{2+}\text{-hGH})_2$ complex serves at least two functions. First, the Zn^{2+}-hGH dimer is more stable to denaturation by guanidine-HCl (Gu-HCl) than monomeric hGH. For example, in the presence of $ZnCl_2$, the concentration of Gu-HCl at which 50% of the hGH is denatured increases from 4.1 M to 4.8 M (Fig. 6). The total amount of hGH released per day in pulses from the pituitary in a growing child is about 50 to 100 nmol; yet the total content of hGH in the pituitary is about 200 to 400 nmol (*1*). Thus, the hormone may be stored for days in vesicles before it is released. Our studies suggest that the $(Zn^{2+}\text{-hGH})_2$ complex in vesicles should be substantially more resistant to denaturation during storage.

Second, the concentration of hGH when released from the pituitary is above 1 mM (*14*), yet by the time it reaches receptors in the periphery, its peak concentration is about 2 nM (*15*), nearly a 10^6-fold dilution. Many cell types contain hGH or human prolactin (hPRL) receptors. This enormous concentration gradient could saturate cellular receptors proximal to the pituitary. However, receptor binding epitopes on hGH for both the hGH receptor (*16*) and hPRL receptor (*17*) are covered in the $(Zn^{2+}\text{-hGH})_2$ complex (Fig. 5). Therefore, the hormone may not become available until the hGH concentration approaches its dimerization dissociation constant (~3 μM), and the $(Zn^{2+}\text{-hGH})_2$ complex may dampen stimulatory effects that could arise from locally high concentrations of hGH near the pituitary gland.

Zn^{2+}-induced hormone oligomerization may modulate in a reversible fashion the stability and activity of other somato-lactogenic hormones. For example, human placental lactogen, which is 85% identical to hGH, has been shown to bind to the hPRL receptor in a Zn^{2+}-dependent fashion (*18*) and contains His^{18}, His^{21}, and Glu^{174}. Most prolactins aligned to hGH contain His^{18}, His^{21}, and Asp^{174} (*19*). Addition of small amounts of Zn^{2+} will dimerize human placental lactogen or precipitate hPRL at concentrations of hormone and metal above about 10 μM (*20*). Furthermore, nonprimate growth hormones contain Gln^{18}, His^{21}, and Glu^{174}. Although glutamine is not a known ligand for Zn^{2+} in proteins, amides can coordinate metals. Alternatively, all nonprimate growth hormones contain

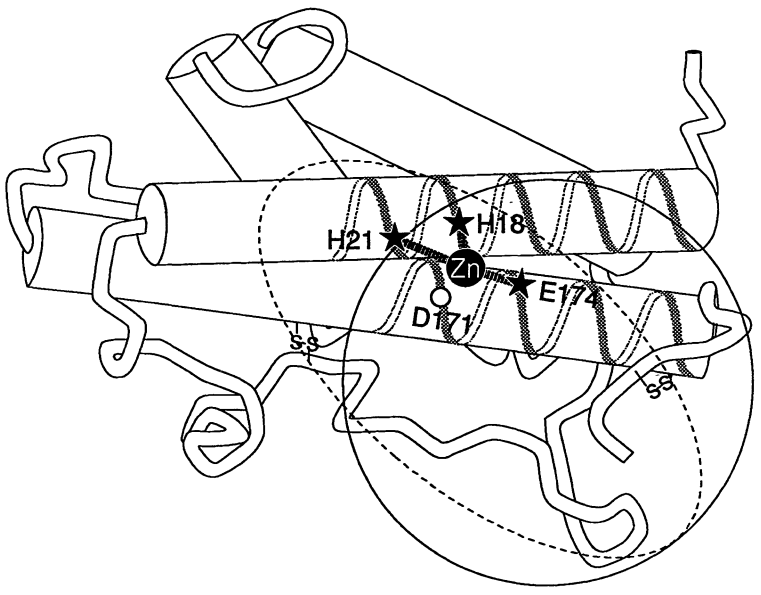

Fig. 5. Location and structure of the Zn^{2+} binding site. Folding model for hGH based upon a 2.8 Å structure of porcine GH (*23*) that shows the putative location of the Zn^{2+} ligands (starred) and binding regions for the extracellular domains of the hPRL (dashed ellipse) and hGH (large solid circle) receptors. Asp^{171} is shown with a small circle, and it is not a ligand. Disulfide bridges are also included.

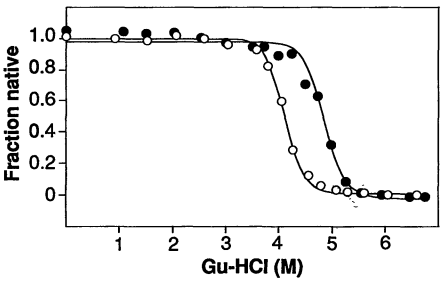

Fig. 6. Stability of hGH to denaturation by Gu-HCl in the presence (●) or absence (○) of 25 μM $ZnCl_2$. A solution containing hGH (30 μg); tris buffer, pH 8.0 (0.01 M); and the indicated Gu-HCl concentration with or without $ZnCl_2$ (25 μM) was equilibrated for 2 min at 25°C before we measured the molar ellipticity at 222 nm (θ_{222}) in a 1-cm circular dichroism cell. Additions of $ZnCl_2$ were made before the Gu-HCl. The fraction hGH folded was calculated from the fractional change in θ_{222} in the absence of Gu-HCl (hGH folded) relative to that in Gu-HCl (6.5 M) (hGH unfolded).

His^{171}, and it is conceivable this serves the role of the missing His^{18}. Finally, our studies suggest a means of improving the stability of hGH by including Zn^{2+} in pharmaceutical preparations and for engineering Zn^{2+} dimers of other helical hormones and proteins.

REFERENCES AND NOTES

1. W. F. Daughaday, in *Textbook of Endocrinology*, J. D. Wilson and D. W. Foster, Eds. (Saunders, Philadelphia, ed. 7, 1985), pp. 577–613.
2. U. J. Lewis, *Annu. Rev. Physiol.* **46**, 33 (1984).
3. O. Thorlacius-Ussing, *Neuroendocrinology* **45**, 233 (1987).
4. F. La Bella, R. Dular, S. Vivian, G. Queen, *Biochem. Biophys. Res. Commun.* **52**, 786 (1973).
5. A. W. Root, G. Duckett, M. Sweetland, E. O. Reiter, *J. Nutr.* **109**, 958 (1979).
6. M. Y. Lorenson, D. L. Robson, L. S. Jacobs, *J. Biol. Chem.* **258**, 8618 (1983).
7. B. C. Cunningham, S. Bass, G. Fuh, J. A. Wells, *Science* **250**, 1709 (1990).
8. G. K. Ackers and T. E. Thompson, *Proc. Natl. Acad. Sci. U.S.A.* **53**, 342 (1965).
9. B. C. Cunningham, M. G. Mulkerrin, J. A. Wells, unpublished results.
10. I. Bertini and C. Luchinat, *Adv. Inorg. Biochem.* **6**, 71 (1984).
11. M. T. Martin, B. Holmquist, J. F. Riordan, *Inorg. Chem.* **36**, 27 (1989).
12. T. Handel and W. F. DeGrado, *J. Am. Chem. Soc.* **112**, 6710 (1990); L. Regan and N. D. Clarke, *Biochemistry* **29**, 10878 (1990).
13. B. L. Vallee and D. S. Auld, *Proc. Natl. Acad. Sci. U.S.A.* **87**, 220 (1990).
14. The Zn^{2+} content of a rat pituitary is estimated to be 75 to 100 ng of Zn^{2+} per milligram of dry pituitary mass (*3*). A normal human pituitary is about 1 ml in volume, of which 65% is water. We estimate there are 350 to 400 nmol of Zn^{2+}, compared with 225 to 450 nmol of hGH (*1*). Roughly 30% of the cells in the pituitary are somatotrophs and in these somatotrophs vesicles account for about 30% of the cell volume (*1*). Thus, the total concentrations of Zn^{2+} and hGH in these vesicles are about 4 to 5 mM and 2.5 to 5 mM, respectively.
15. A. L. Taylor, J. L. Finster, D. H. Mintz, *J. Clin. Invest.* **48**, 2349 (1969); R. G. Thompson, A. Rodriguez, A. Kowarski, R. M. Blizzard, *ibid.* **51**, 3193 (1972); K. Y. Ho *et al.*, *J. Clin. Endocrinol. Metab.* **64**, 51 (1987).
16. B. C. Cunningham and J. A. Wells, *Science* **244**, 1081 (1989).
17. ———, *Proc. Natl. Acad. Sci. U.S.A.* **88**, 3407 (1991).
18. H. B. Lowman, B. C. Cunningham, J. A. Wells, *J. Biol. Chem.* **266**, 10982 (1991).
19. C. S. Nicoll, G. L. Mayer, S. M. Russell, *Endocr. Rev.* **7**, 169 (1986).
20. H. B. Lowman and J. A. Wells, unpublished data.
21. D. A. Yphantis, *Biochemistry* **3**, 297 (1964).
22. S. J. Shire, L. A. Holladay, E. Rinderknecht, *ibid.*, in press.
23. S. S. Abdel-Meguid *et al.*, *Proc. Natl. Acad. Sci. U.S.A.* **84**, 6434 (1987).

24. We thank S. Shire for advice and help with sedimentation equilibria studies; L. Holladay for providing the computer program to fit the sedimentation equilibria data and calculate dimerization constants; B. Kelley for advice on equilibrium dialysis experiments; S. Spencer, T. Bewley, and T. Kossiakoff for critical reading of the manuscript; and W. Anstine for preparation of graphics and the manuscript.

11 March 1991; accepted 23 May 1991

Predictable Upwelling and the Shoreward Transport of Planktonic Larvae by Internal Tidal Bores

JESÚS PINEDA

Internal tidal bores have a crucial role in the transport of drifting larvae to marine nearshore populations, a key factor in structuring benthic communities. Shoreward transport of larvae and abrupt surface temperature drops lasting days can be explained by invoking the advection of subsurface cold water to the shore by internal tidal bores. This process is predictable within the lunar cycle and brings deep water to the surface (upwelling) in a direction perpendicular to the coastline.

KNOWLEDGE OF TRANSPORT MECHanisms perpendicular to the coastline is essential to understanding the exchange of material and water properties between the nearshore and the coastal ocean; an important ecological example is the problem of the supply of pelagic larvae to intertidal and shallow habitats. The supply of recruits to benthic populations has long been recognized as a critical factor in structuring benthic communities (*1*). The rate at which planktonic larvae establish permanent contact with the substratum (settlement rate) (*2*) occasionally shows a wave form input. This pattern of settlement has been correlated with the onshore transport of barnacle and crab larvae by surface slicks generated by internal waves (*3*) and wind-induced currents (sometimes associated with synchronous offspring release) (*4–6*). Processes governing the transport of larvae are similar to those influencing the redistribution of water properties. Abrupt surface water temperature drops during the summer in the Southern California Bight have been traditionally attributed to wind-driven Ekman upwelling (*7, 8*); however, most studies have been inferential (*9*), and there is only weak atmospheric forcing in the summer (*10*). Here it is proposed that the summer temperature drops visible in the Scripps Pier daily surface water temperature and the transport of planktonic larvae of nearshore organisms shoreward are both well explained by the advection of subsurface cold water (upwelling) resulting from predictable internal tidal bores.

In a manner similar to surface waves, internal waves change as they approach the shore. When wave amplitude becomes non-negligible with respect to water depth, the wave becomes asymmetrical; the leading edge steepens, the trailing edge flattens, and it propagates forward as an internal bore (*11, 12*). Internal waves (*13, 14*) and bores (*12, 15*) of tidal periodicity have frequently been observed in summer in the Southern California Bight. In fall and winter the water column within the Bight is typically weakly stratified and internal motions are much less energetic (*14, 16*). A spring-neap surface tidal cycle suggests an internal tidal spring-neap cycle, as some claim to have observed (*17*). The internal tide, however, is not consistently in phase with the surface tide (*13, 14*). Passing internal waves produce vertical water displacements which can be recorded with fixed temperature sensors if the water column is thermally stratified. Thermal changes close to the bottom occurring in short time spans (on the order of 2° to 5°C over minutes) are salient features of internal bores and might indicate horizontal advection of water (figure 1 in *12, 15*). Water temperature sensors were installed at two depths at the end of the Scripps Pier in August 1989. Large diurnal or semidiurnal fluctuations in bottom water temperature reveal internal tidal bores (Fig. 1). The hourly record shows that internal bores are ubiquitous in the summer, but they appear more infrequent in the fall portion of the record (Fig. 1A). Small-event internal bores are characterized by a layer of cold water restricted in its distance from the bottom (Fig. 1B, 5 August at about 3 a.m.). In the less frequent, large-event bores the cold water occurs from the bottom to the surface sensors (Fig. 1B, 8 August at about 2 p.m.; Fig. 1A, 20 to 24 August); in some cases, coinciding with the arrival of the bore, the surface temperature remains low for days (Fig. 1B); in others, lower and higher surface water temperatures occur alternately at apparently diurnal or semidiurnal periodicity without a persistent lowering of the surface temperature (Fig. 1A, 20 to 24 August). The data in Fig. 1 support the

Scripps Institution of Oceanography, La Jolla, CA 92093–0208.